Research Article

Gültekin Basmacı*, Mevlüt Yunus Kayacan, Mustafa Ay, Ayhan Etyemez

Optimization of cutting forces and surface roughness via ANOVA and grey relational analysis in machining of In718

https://doi.org/10.1515/chem-2022-0273
received December 5, 2022; accepted December 22, 2022

Abstract: Machinability and optimization are the two objectives of researchers who guide us to enhance the manufacturing industry. Examining and analyzing the parameters such as surface roughness, tool wear, and cutting force during the processing would be beneficial that are used in various fields in the manufacturing industires. This study examined the effect of cutting forces to surface roughness on the material surface. Experimental studies were carried out by using constant feed rate (0.1 mm/rev), depth of cut (1 mm), three different coolants (CO_2, minimum quantity lubrication, and dry), and cutting speeds (100, 140, 180, 220 m/min). In this study, grey relational analysis modeling and analysis of relationships between F_x, F_y, and F_z forces on the surface roughness of Inconel 718 material, which is an important alloy in aviation, is examined. The influence of machinability parameters on F_{top} and R_a was calculated using variance analysis, which determined that cutting speed was the most significant machining parameters.

Keywords: surface roughness, Inconel 718, machinability, Taguchi, optimization, grey relation, ANOVA

1 Introduction

Because of cost, product quality, and other parameters which are significant factors for utilization areas, material choice, and production rate, metal cutting efficiency and machine parameter optimization have become increasingly important as the manufacturing industry has grown significantly. One of the most broadly adopted machining processes for transforming a material into the required geometric shape is machining. The problematic areas are machined with a cutting tool that is harder and tougher than the material throughout the cutting process. High cutting forces resulting from friction between the cutting tool and the material surface have a direct impact on tool life and surface quality. The heat generated during the chip removal operation should be managed to prolong the life of the cutting tool and improve the surface quality of the materials [1–4].

Becasue of their chemical and physical attributes, superalloys are difficult to process, but they are highly preferred materials [5–7]. Furthermore, the machinability, hardness, as well as other properties of materials can be modified by introducing elements such as sulfur and selenium into composition [8–11]. These materials are composed of nickel–iron and one of the base superalloys, Inconel 718 (2.4668), is employed in a variety of critical applications [12]. Owing to the elements added to the Inconel 718 alloy, it gains properties such as high temperature, corrosion, cracking, and fatigue characteristics, whereas these elements make Inconel's machinability more difficult and increase the machining cost. Many academic studies have been undertaken in recent years to investigate the effects of cutting parameters on cutting forces and surface roughness that occur during the machining of Inconel 718. High temperature, cutting tool wear, and chemical reaction susceptibility between the cutting tool and the material during the cutting process are the key issues encountered while machining Inconel 718 [13]. Machinability of superalloy materials in manufacturing can be

* **Corresponding author: Gültekin Basmacı,** Department of Mechanical Engineering, Faculty of Engineering and Architecture, Mehmet Akif Ersoy University, Burdur, Turkey, e-mail: gbasmaci@mehmetakif.edu.tr
Mevlüt Yunus Kayacan: Technology Faculty, Mechanical Engineering, Isparta University of Applied Sciences, Isparta, Turkey
Mustafa Ay: Department of Mechanical Engineering, Faculty of Technology, Marmara University, Istanbul, Turkey
Ayhan Etyemez: Department of Mechanical Engineering, Faculty of Technology, Marmara University, Istanbul, Turkey

improved through appropriate parameter assessment, cutting tool configuration, and lubrication methods, among many other things. During the cutting of the material, rpm, feed rate, depth of cut, and other parameters are described in the literature. When reviewing studies on the effects of parameters, Swamy et al. found that cutting tool wear is less between 225 and 450 rpm, and the surface roughness decreases as the rpm increases in their study on Alloy (Inconel) 718. He also noticed that when the feed rate was increased from 0.1 to 0.3 mm, the surface roughness (R_a) increased dramatically [14]. Panadian and Rout deployed a carbon-coated drill as a cutting tool on Inconel 718 and established that the surface roughness (R_a) decreased with higher cutting speed (700 rpm), feed rate (20 mm/min), and low depth of cut (0.2 mm). They further demonstrated that a low cutting speed (500 rpm) and a depth cut (0.4 mm) resulted in minimum cutting tool wear [15]. Due to its low heat conductivity, Inconel 718 can achieve high temperatures of 900–1,300°C during manufacturing. Throughout machining, the insert is exposed to these high temperatures, bringing challenges with surface topography and dimensional accuracy, as well as a significant decrease in tool life [16,17].

While determining the most efficient cutting parameters for sustainable machining and limited resources in our world, it is essential to identify optimum parameters. The grey relational analysis (GRA) method, one of the optimization approaches, determines the optimum values of the parameters, which are calculated with an accuracy rate depending on the percentage of experiments. The influence of the parameters that should be performed to achieve the intended material integrity was investigated in research focusing on these outcomes, and they concluded that the feed rate was 63.7% performance parameters, the depth of cut was 19% effective, and the cutting speed was 6.9% effective. The grey relational grade (GRG) score improved by 0.563 points as a result of the confirmation experiment conducted upon those data [18,19]. Based on the results of the validation experiments they executed as a result of the grey analysis, Ramesh et al. stated that feed rate, cutting speed, and depth of cut had also grown massively in material quality [20]. The cutting parameters have been optimized using a variety of approaches, including CCD, RSM, ANN, and GRA. According to Ma et al. energy consumption, surface roughness, and machining duration can all be minimized by 4–40% by optimizing the cutting conditions while processing the material [21]. As a result of the GRA analysis they performed on Pekşen and Kalyon AISI 430 stainless steel, the GRG values increased by 0.387, creating a great effect of 69.1% [22]. There are many studies in the literature regarding the machining of metals under cryogenic conditions. However, in contrast to metals, studies in relation to the optimazation of machining super alloys are limited.

In this study, Inconel 718 was assessed at several cutting speeds (100–140–180–220 rpm) and with three different coolants (dry stock removal, CO_2, and minimum quantity lubrication [MQL]). Afterward, utilizing GRA, ANOVA, and regression methods, the influences of these variables on cutting forces and surface roughness were determined, and optimization was performed.

2 Materials and methods

The material used throughout the experiment was Inconel 718 super alloy, which has a diameter of 50 mm and a length of 200 mm. Table 1 summarizes the chemical specifications of the material investigated in this research. Nickel, iron, and chromium are the primary components of Inconel 718, as can be seen in the composition. As a result, it generates a hard alloy with a low convection coefficient and a high heat resistance [23].

MQL provides a balanced lubricant and air mixture as well as a very low aerosol spray to the machining zone [24,25]. Thirty-two experiments were carried out using the cutting speed and cooling processes that employed, and the determined the force values (F_x, F_y, and F_z) in the X, Y, and Z axes, as well as the surface roughness (R_a) values, were obtained. Figure 1 represents the equipment and experimental setup.

The cutting fluid was mixed with air at 6 bar using a nozzle and an air compressor in the MQL system and afterward supplied to the workpiece-cutting tool interface as shown in Figure 2. The machining experiments utilized three different types of lubricants (dry, MQL, and CO_2), two different lubricant flow rates (20 and 40 mL/h), and four different cutting speeds (100, 140, 180, and 220 m/min). Cutting speeds, depth of cut, and feed rate have been determined according to the tool manufacturer (SUMITOMO). The turning experiments used a constant feed rate f = 0.1 mm/rev and a constant depth of cut at = 1 mm. The manufacturer's suggested handbook was used to select process parameter settings.

Cutting tools were provided from ISO CNMG 12 04 08 MM SUMITOMO. The reason for choosing these tools is that it has been observed in different studies that they have very positive effects on both the flank wear on the cutting edge and the surface quality of the workpiece [14,15,17]. An x–z axis CNC from Johnford and a Mahr

Table 1: Machining input process parameters

Parameters	Workpiece material					
	Inconel 718 (Chemical composition %)					
	Cr	17–21	Mn	0.35 max.	S	0.015 max.
	C	0.08 max.	Si	0.35 max.	Al	0.2–0.8
	Fe	19.03	Mo	2.8–3.3	Cu	0.30 max.
	Co	1 max.	P	0.015 max.	Nb + Ta	4.75–5.5
	Ni	50–55			Ti	0.65–1.15
Cutting tool	CNMG 12 04 08 MM SUMITOMO and CNMG120408-MW5 WPP20S					
Cutting speed (vc)	100–140–180–220 m/min					
Feed (fr)	0.1 mm					
Workpiece dimensions	50 mm dia*200 mm					
Drilling environment	Dry, CO_2, and MQL					
MQL supply	Air: 6.0 bar, Lubricant: 20 –40 mL/h (through external nozzle)					
Response considered	R_a (surface roughness), F_x–F_y–F_z (forces)					

perthometer/M1 type micro-hardness analyzer were included in the experiments. For the cutting force measurement, the Kistler 9121 dynamometer system was used, together with a Kistler 5019 charge amplifier and DynoWare software.

The cutting parameters of the CNC machined Inconel 718 material are listed in Table 2.

Cutting forces were measured during the manufacturing process, and surface roughness values were obtained following this investigation. The data received were then exposed to ANOVA, regression analysis, and GRA processes in order to correlate the factor levels seen in the Taguchi experimental design. Experimental steps has demonstrated in Figure 2.

Classical experimental design methodologies are time-consuming and costly to implement in industrial applications. As a result, it may be quicker and more efficient to use the Taguchi approach to reduce the number of experiments. As a result of pre-experiment investigations, a significant

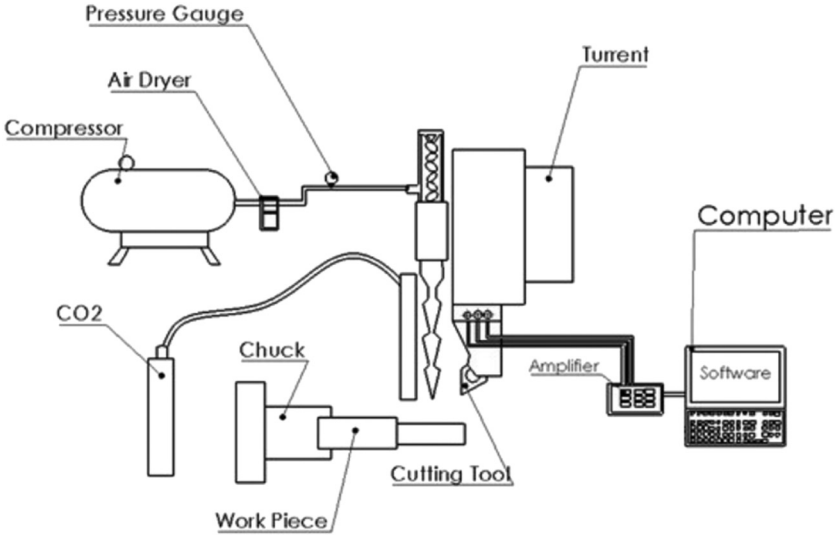

Figure 1: Experimental setup.

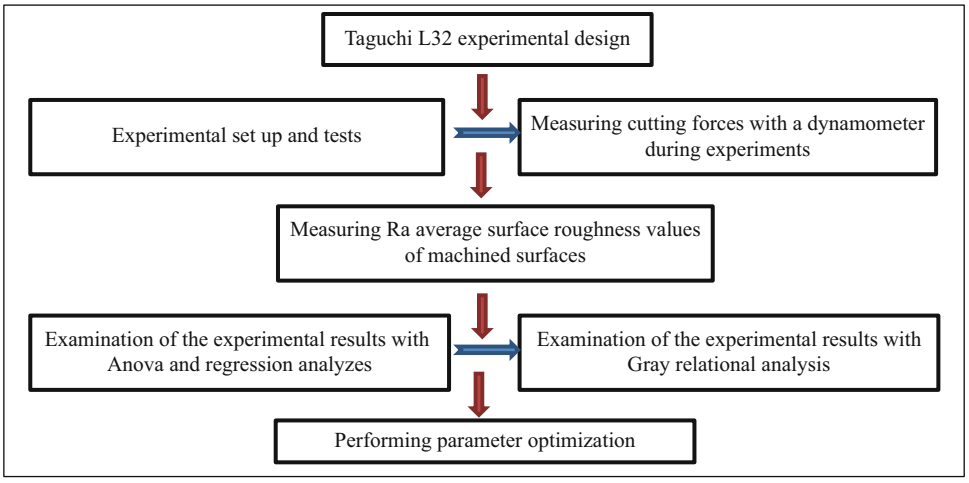

Figure 2: Workflow of the study.

Table 2: Factors and grades in Taguchi experimental design

Parameters	Level 1	Level 2	Level 3	Level 4
Insert	CNMG 12 04 08 MM SUMITOMO	CNMG120408-MW5 WPP2	N/A	N/A
Coolant	Dry	MQL 20 mL/h	MQL 40 mL/h	CO_2
Cutting speed (m/min)	100	140	180	220

decrease in the number of experiments can be accomplished by executing selected experiments instead of full factorial experiments. This method involves assessing an equivalent number of samples for various factor values, with each parameter influencing the results. An orthogonal design was created using Taguchi's experimental design L32, and the factors and levels are listed in Table 2.

The Taguchi experimental data were evaluated by adapting it to a signal-to-noise ratio (S/N). The S/N ratio is the proportion of the experimental results to a factor that has no effect on the experimental design but has an influence on the test results. Because it is important to minimize cutting forces and surface roughness, the maxim "smaller is better" was chosen for this investigation. The following equation was used to calculate the S/N ratio [23]:

$$\frac{S}{N} = -10\log\left[\frac{1}{n}\sum_{i=1}^{n} y_i^2\right]. \tag{1}$$

In addition to the ANOVA method, the GRA approach was also used in parameter optimizations within the scope of the study. GRA is a decision-making method, and the procedures in the calculation can be seen in the following equation:

$$x_0 = (x_0(1), x_0(2), x_0(3), \ldots\ldots\ldots\ldots\ldots x_0(n)). \tag{2}$$

One of the standard operating procedures with normalization approaches is linear data preprocessing. For surface roughness and cutting forces, "smaller is better" normalization was adopted in this investigation. When surface roughness and cutting forces were linearly normalized, values with small ratios would be close to 1 and values with large ratios would be close to 0. A normalization operation was performed under the condition of "smaller is better," as shown in the following equation:

$$X_{i^{(k)}} = \frac{\max(x_i^0(k)) - (x_i^0(k))}{\max(x_i^0(k)) - \min(x_i^0(k))}. \tag{3}$$

The resulting row of the series of length n is represented by the symbol "k." Equations (4) and (5) are used to calculate the grey relationship coefficient at point (k):

$$x_i = (x^i(1), x^i(2), x^i(3), \ldots\ldots\ldots\ldots\ldots, x^i(n)), \quad i = 1, 2, 3, \ldots, m), \tag{4}$$

$$n((x_0k), x_j(k)) = \frac{n_{\min} + \zeta n_{\max}}{n_{0i}(k) + \zeta n_{\max}}. \tag{5}$$

ζ notation is a coefficient between 0 and 1. The ζ notation determines the difference between $n_{0i}(k)$ and $n_{\max}$. Studies show that the ζ ratio does not affect the rating after the GRG calculation. GRG is calculated by the following equation:

Table 3: Experimental results

Test number	Insert	Cutting speed (m/min)	Coolant	F_x	F_y	F_z	F_{top}	R_a
1	1	100	Dry	1,047	658	797	1,471	2.005
2	1	140	Dry	1,042	457	566	1,271	0.365
3	1	180	Dry	1,052	517	511	1,279	0.693
4	1	220	Dry	895	524	401	1,112	0.649
5	1	100	MQL 20 mL/h	1,026	446	635	1,286	2.051
6	1	140	MQL 20 mL/h	990	517	633	1,283	0.37
7	1	180	MQL 20 mL/h	1,023	491	548	1,260	0.74
8	1	220	MQL 20 mL/h	781	422	404	975	1.45
9	1	100	MQL 40 mL/h	1,018	506	786	1,382	0.346
10	1	140	MQL 40 mL/h	1,094	537	728	1,419	0.925
11	1	180	MQL 40 mL/h	1,017	503	539	1,256	0.331
12	1	220	MQL 40 mL/h	756	457	392	966	0.527
13	1	100	CO_2	960	468	564	1,208	1.96
14	1	140	CO_2	1,136	464	794	1,461	1.65
15	1	180	CO_2	954	442	633	1,227	1.284
16	1	220	CO_2	835	559	609	1,175	2.684
17	2	100	Dry	997	507	725	1,332	0.671
18	2	140	Dry	617	369	438	842	1.345
19	2	180	Dry	618	430	481	893	0.994
20	2	220	Dry	463	282	302	621	0.381
21	2	100	MQL 20 mL/h	951	608	606	1,281	0.323
22	2	140	MQL 20 mL/h	763	416	392	953	0.299
23	2	180	MQL 20 mL/h	520	347	263	679	0.288
24	2	220	MQL 20 mL/h	415	267	202	533	0.834
25	2	100	MQL 40 mL/h	914	391	655	1,191	2.199
26	2	140	MQL 40 mL/h	906	441	577	1,161	0.844
27	2	180	MQL 40 mL/h	582	340	389	778	0.39
28	2	220	MQL 40 mL/h	453	322	326	645	0.551
29	2	100	CO_2	814	397	562	1,066	1.382
30	2	140	CO_2	746	402	511	990	1.059
31	2	180	CO_2	554	429	482	850	0.962
32	2	220	CO_2	406	255	403	626	1.212

$$\gamma(\mathrm{x}_0, \mathrm{x}_i) = \left[\frac{1}{n} \sum_{n}^{k=1} n(x_0(k), x_j(k)) \right]. \quad (6)$$

The proper experiments that would produce the conditions where the R_a and F_{top} values would be the minimum could be listed by sorting the coefficients acquired with the GRG according to "the smallest is better." Idealized parameters comprising two result functions and two optimization procedures were identified, and the three best experimental parameters were determined and compared with the ANOVA analysis.

3 Results and discussions

Cutting forces were measured using a dynamometer, which can collect force data in three axes while machining. The surface roughness of the processed materials was then calculated as R_a. It has been discovered that cutting forces and surface roughness might well be minimized by maintaining the machining parameters at optimal values. R_a values were evaluated following machining processes in this investigation. According to the literature, the 1 mm chip amount provided adequate surface quality [26,27]. For each cutting process, a new, non-reused cutting tool was chosen. To generate realistic surface roughness values, roughness values were averaged for different areas of the surface.

Taguchi L32 was performed within the scope of the investigation using a mixed-type experimental design. Machinability experiments were conducted utilizing two different cutting tools, four different coolants, and four different cutting rates. For the same type of material, all experiments were accomplished by subtracting the same amount of materials. Table 3 represents the test results. In Table 3, meanings of forces are F_x feed force, F_y radial force, and F_z cutting force.

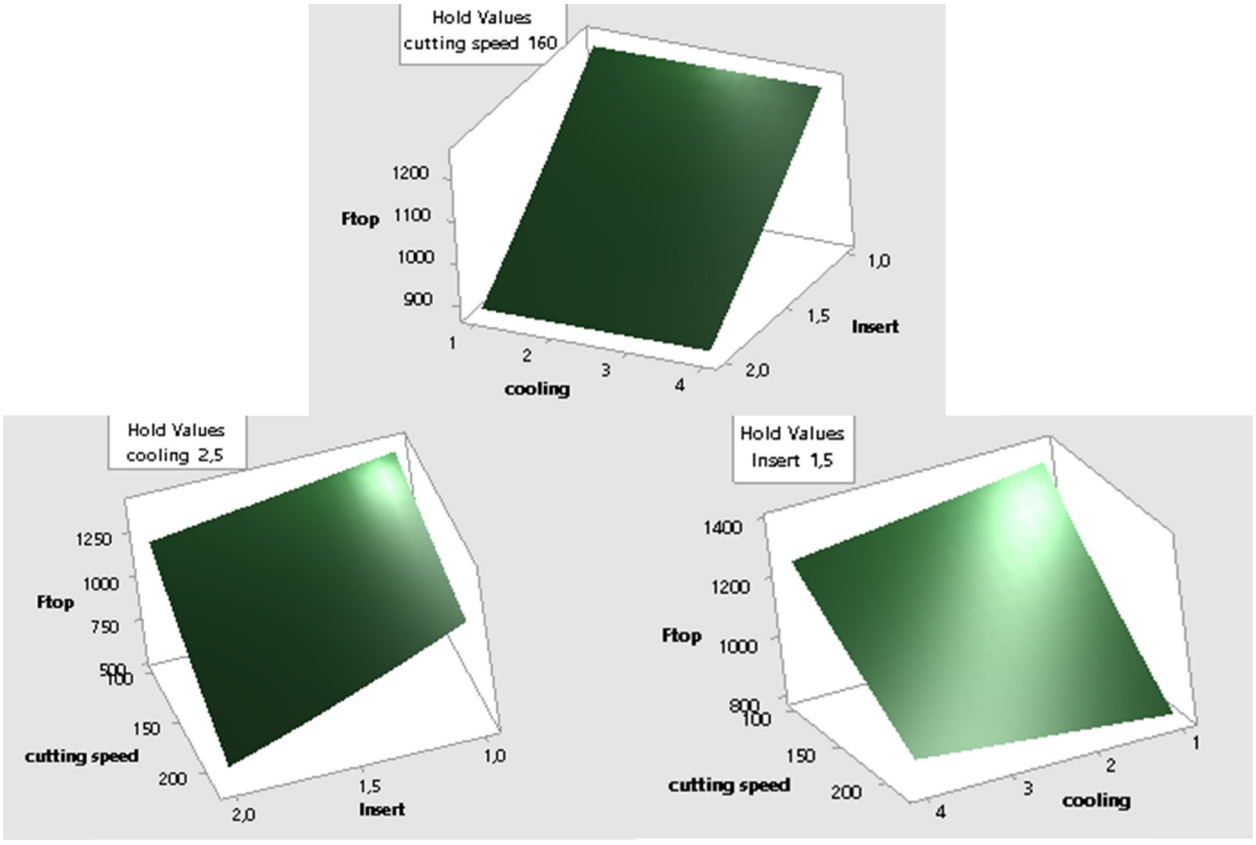

Figure 3: Relation of resultant cutting forces with machinability parameters.

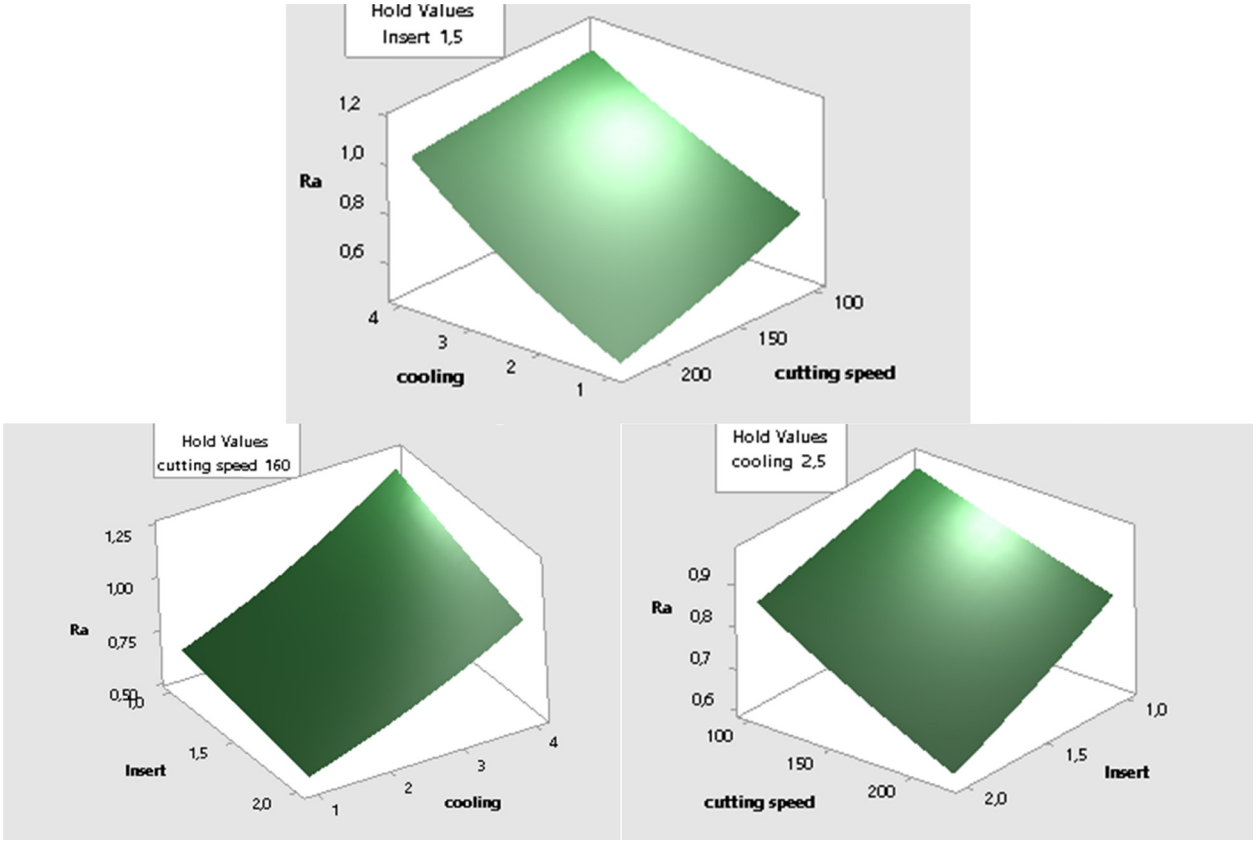

Figure 4: Relation of surface roughness with machinability parameters.

Table 4: ANOVA results for F_{top}

Input	DF	SS	MS	*F* ratio	PCR%
Coolant*cutting speed	3	79.21	26.402	10.48	14.74
Cutting speed	3	48.78	16.261	6.45	9.07
Coolant	1	18.43	18.433	7.31	3.43
Cutting tool	1	247.11	247.114	98.04	45.97
Coolant*Coolant*cutting tool	3	98.4	32.801	13.01	18.31
Coolant*cutting tool	1	18.37	18.368	7.29	3.42
Cutting speed * cutting tool	3	27.23	9.077	3.6	5.07
Error	16	40.33	2.521		
Total	31	577.87			100

3.1 ANOVA and regression analyses

In the test results, resultant cutting forces F_{top} were found to be in the range between 553 and 1,471 N. Simultaneously, the surface roughness R_a varied between 0.288 and 2.199 μm. Cutting speed, cutting tool, and coolant had an effect on alterations in cutting forces and surface roughness values. The effects of the parameters on the findings were determined within the scope of the study employing ANOVA and regression analyses. The R2 regression value of cutting forces was calculated to be 93.02%. The surface roughness R^2 was calculated to be 94.66%. Figures 3 and 4 show the relationship between cutting forces and surface roughness with parameters as a consequence of these experiments.

It has been discovered that the type of cutting tool has the biggest influence on cutting forces. The coolant with the lowest effect was selected. Cutting speeds have a smaller effect compared to cutting tool types. On the other hand, it has been determined that the coolant has a significant effect on the surface roughness, which is the inverse of the cutting forces. The surface roughness was also significantly affected by the tool geometry type and cutting speeds. Nonlinear parameters that may have an effect on F_{top} and R_a were defined in addition to those variables for ANOVA analysis. As a result, the opportunity to improve the performance of the analysis was found. ANOVA analysis was used to evaluate the effect of the parameters for the cutting forces, as shown in Table 4. As seen in Figure 4, the ANOVA analysis exposed that the cutting tool had the biggest impact on the cutting forces. Moreover, the nonlinear parameters such as "Coolant*Coolant*cutting tool" and "Coolant*cutting speed" influenced the difference in cutting forces significantly.

Nonlinear parameters have been determined for R_a as well as for determining the parameters affecting the cutting forces. The ANOVA analysis results for surface roughness are given in Table 5. The three parameters that have the greatest effect on the surface roughness were determined as coolant, "coolant*cutting tool," and "coolant*cutting speed." It has been observed that ANOVA analyses with dependent variables have similarly performed in recent studies [28]. Coolant is a dependent variable, like nonlinear parameters. The linear or nonlinear dependent properties of the cutting forces have essentially little effect on the surface roughness.

The effects of machinability parameters on R_a and F_{top} with models produced by ANOVA and regression analyses are shown in Figure 5. According to the results, the changes in cutting tools and coolants caused similar changes on R_a and F_{top}. At the same time, increasing cutting speeds resulted in a decrease in R_a and an increase in F_{top}.

The analysis of the S/N curves are obtained and displayed in Figure 6. It has been understood that the surface roughness of R_a changes at high rates with the

Table 5: ANOVA results for R_a

Input	DF	SS	MS	*F* ratio	PCR%
Coolant*cutting speed	9	1.05	0.12	0.46	23.50
Cutting speed	3	0.33	0.11	0.44	7.42
Coolant	3	1.33	0.44	1.76	29.78
F_x	1	0.05	0.05	0.22	1.21
F_y	1	0.05	0.05	0.2	1.09
F_z	1	0.06	0.06	0.25	1.41
F_{top}	1	0.09	0.09	0.34	1.90
F_x* F_x	1	0.14	0.14	0.57	3.22
F_y* F_y	1	0.03	0.03	0.12	0.67
F_z* F_z	1	0.07	0.07	0.27	1.50
F_{top}* F_{top}	1	0.04	0.04	0.16	0.92
Cutting tool	3	0.37	0.37	1.47	8.27
Coolant*cutting tool	3	0.64	0.22	0.85	14.37
Cutting speed* cutting tool	1	0.21	0.07	0.28	4.76
Error	1	0.25	0.25		
Total	31	4.74			100

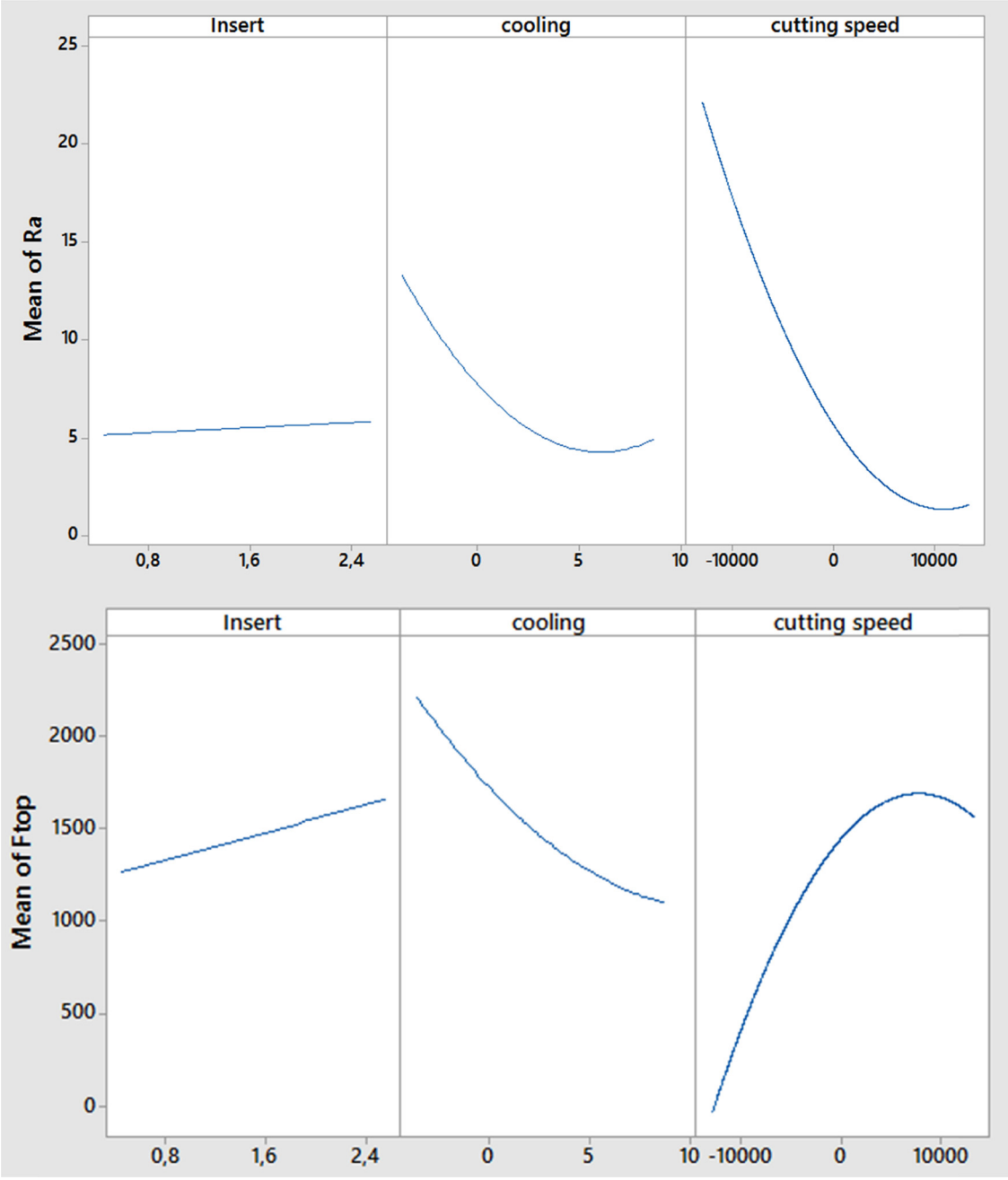

Figure 5: Effect of machinability parameters on F_{top} and R_a.

change of the coolant, and the effect of the change in the cutting tool type on R_a was the lowest. Obtained data were also consistent with previous results.

The purpose of the optimization research conducted after the ANOVA analysis is to minimize the R_a and F_{top} values. According to the investigation, the optimum cutting force and surface roughness were obtained at 220 m/min cutting speed and 40 mL/h MQL cooling conditions for both cutting tools. F_{top} and R_a were obtained as 805 N and 0.797 µm, respectively, using optimal parameters. The optimal roughness values for In718 material have been determined to be higher than the machining procedures in recent years [19,29]. ANOVA optimization study is presented in Figure 7.

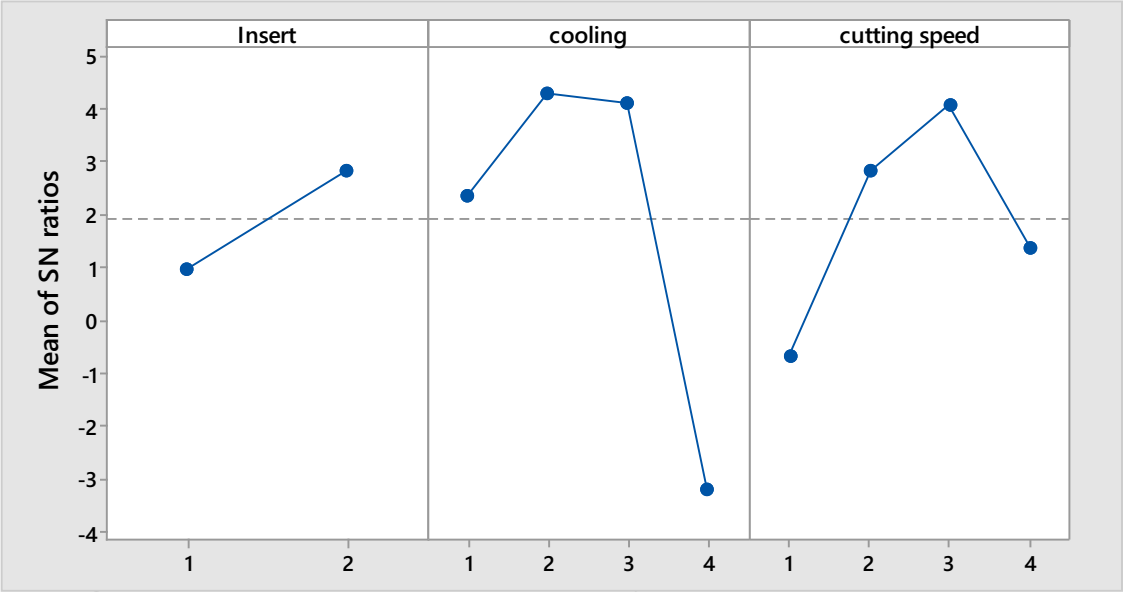

Figure 6: S/N ratios of R_a for machinability parameters.

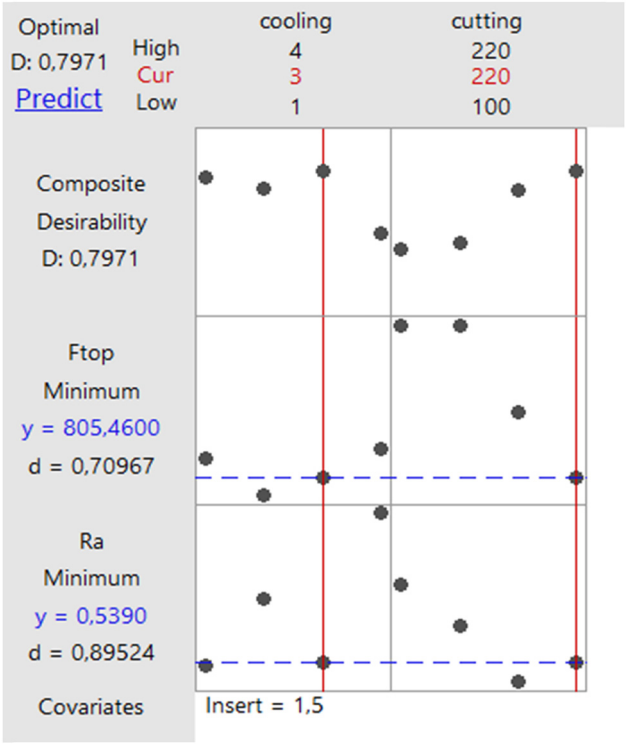

Figure 7: ANOVA optimization results.

3.2 GRA

The GRA approach was used in this study to determine the optimal parameters based on the machinability criteria and surface roughness of Inconel 718 nickel-based superalloy. The aim is to decrease both F_{top} and R_a values. Normalization techniques were used to generate grey correlation coefficients, and performance rankings were derived by comparing 32 experiments. Table 6 shows the GRA coefficients, S/N ratios, and success rankings based on the test results for all studies. Examining the parameters of the three best tests demonstrated that the cutting tool No. 2, cutting speed of 220 m/min, and cooling conditions with 20 mL/h MQL exposed the best results. F_{top} and R_a were, respectively, calculated as 611 N and 0.501 µm.

When both the ANOVA analysis and the GRA data were considered, it was concluded that a cutting speed of 220 m/min and MQL cooling conditions were appropriate. GRA resulted in 59% better R_a and 31% better F_{top} outcomes. The parameters influencing surface roughness and cutting forces were established by reviewing the GRG values and delta data obtained with GRA. The GRG analysis is shown in Table 7. It has been observed that cutting speed has a greater impact on the results than cutting tool type and coolant. A similar result was found in the literature studies and the ANOVA analysis [30,31]. It is also important that interesting results were obtained in some other works [32–52].

4 Conclusions

Machinability experiments on Inconel 718 nickel-based superalloy were performed in this article, considering

Table 6: Results of GRA

Exp. no.	Experimental F_{top}	Experimental R_a	Grey relational coeff. F_{top}	Grey relational coeff. R_a	GRG	S/N ratio	Rank
1	1,471	2.005	0.333	0.411	0.372	−6.042	32
2	1,271	0.365	0.389	0.940	0.664	8.754	11
3	1,279	0.693	0.386	0.747	0.567	3.185	18
4	1,112	0.649	0.447	0.768	0.608	3.755	15
5	1,286	2.051	0.384	0.405	0.394	−6.239	30
6	1,283	0.370	0.385	0.936	0.660	8.636	12
7	1,260	0.740	0.392	0.726	0.559	2.615	20
8	975	1.450	0.515	0.508	0.511	−3.227	23
9	1,382	0.346	0.356	0.954	0.655	9.218	13
10	1,419	0.925	0.346	0.653	0.499	0.677	24
11	1,256	0.331	0.393	0.965	0.679	9.603	8
12	966	0.527	0.520	0.834	0.677	5.564	10
13	1,208	1.960	0.410	0.417	0.414	−5.845	27
14	1,461	1.650	0.336	0.468	0.402	−4.350	28
15	1,227	1.284	0.403	0.546	0.475	−2.171	26
16	1,175	2.684	0.422	0.333	0.378	−8.576	31
17	1,332	0.671	0.370	0.758	0.564	3.466	19
18	842	1.345	0.603	0.531	0.567	−2.574	17
19	893	0.994	0.566	0.629	0.598	0.052	16
20	621	0.381	0.842	0.928	0.885	8.382	1
21	1,281	0.323	0.385	0.972	0.678	9.816	9
22	953	0.299	0.527	0.991	0.759	10.487	7
23	679	0.288	0.763	1.000	0.882	10.812	2
24	533	0.834	1.000	0.687	0.843	1.577	3
25	1,191	2.199	0.416	0.385	0.401	−6.845	29
26	1,161	0.844	0.428	0.683	0.555	1.473	22
27	778	0.390	0.657	0.922	0.789	8.179	5
28	645	0.551	0.808	0.820	0.814	5.177	4
29	1,066	1.382	0.468	0.523	0.495	−2.810	25
30	990	1.059	0.507	0.608	0.558	−0.498	21
31	850	0.962	0.596	0.640	0.618	0.336	14
32	626	1.212	1.000	0.565	0.782	−1.670	6

Table 7: Response table for GRG

Input	Level 1	Level 2	Level 3	Level 4	Delta
Cutting tool	0.5321	0.6743	N/A	N/A	0.1422
Coolant	0.6031	0.6609	0.6337	0.5152	0.1457
Cutting speed	0.4967	0.5831	0.6458	0.6873	0.1906
Total mean GRG	0.6032				

the cutting speed, cutting tool type, and coolant. The analysis was used to optimize the parameters by comparing the experimental results and the established models. It has been determined that the results acquired from the developed models and the experimental results are completely inclusive. Surface roughness and cutting forces were used to guide the investigations. In the experiments, ANOVA, regression analysis, and the GRA method were performed. In tests 20, 23, and 24, which were completed in accordance with the L32 Taguchi design, results were achieved in which R_a and F_{top} were both minimized. Cutting speeds have the highest effect on the results, and the optimum was determined as 220 m/min. Coolant and cutting tool types had similar weight results and were optimized as 20 mL/h MQL and tool type 2, respectively. However, it was determined that the surface roughness and cutting forces were improved at high levels by using the optimized parameters of the Taguchi-assisted GRA analysis. According to the results, the processing of Inconel 718 superalloys shows that the performance values can be improved significantly in further studies by using GRA and ANOVA in the literature. Processing cutting speeds at higher levels to improve surface roughness concerning optimization is in line with studies in the literature.

Funding information: There is no funding for this article.

Author contributions: The contributions of the authors are equal.

Conflict of interest: Authors have declared no conflict of interest.

Ethical approval: The conducted research is not related to either human or animal use.

Data availability statement: The datasets generated during and/or analyzed during the current study are available from the corresponding author on reasonable request.

References

[1] Payal H, Maheshwari S, Bharti PS. Parametric optimization of EDM process for Inconel 825 using GRA and PCA approach. J Inf Optim Sci. 2019;40(2):291–307.
[2] Shen Y, Liu Y, Dong H, Zhang K, Lv L, Zhang X, et al. Surface integrity of Inconel 718 in high-speed electrical discharge machining milling using air dielectric. Int J Adv Manuf Technol. 2016;90(1–4):691–8.
[3] Das SR, Panda A, Dhupal D. Experimental investigation of surface roughness, flank wear, chip morphology and cost estimation during machining of hardened AISI 4340 steel with coated carbide insert. Mech Adv Mater Mod Process. 2017;3(1):9.
[4] Zhou J, Ren J, Yao C. Multi-objective optimization of multi-axis ball-end milling Inconel 718 via grey relational analysis coupled with RBF neural network and PSO algorithm. Measurement. 2017;102:271–85.
[5] Chakraborty S, Bose D. Improvement of die corner inaccuracy of Inconel 718 alloy using entropy based GRA in WEDM process. Adv Eng Forum. 2017;20:29–41. doi: 10.4028/www.scientific.net/AEF.20.29.
[6] Machno M, Matras A, Szkoda M. Modelling and analysis of the effect of EDM-drilling parameters on the machining performance of Inconel 718 using the RSM and ANNs methods. Materials (Basel). 2022 Feb;15(3):1152.
[7] Kumar AK, Venkataramaiah P. Experimental investigation on surface integrity of Inconel 718 under hot machining and optimisation of its process parameters. Adv Mater Process Technol. 2021;1:1–13.
[8] Srinivasulu Reddy K, Venkata Reddy V, Mandava RK. Optimization of turning process parameters using entropy-GRA and DEAR methods. In Lecture Notes in Mechanical Engineering. Singapore: Springer Singapore; 2021. p. 315–24.
[9] Danish M, Gupta MK, Rubaiee S, Ahmed A, Korkmaz ME. Influence of hybrid Cryo-MQL lubri-cooling strategy on the machining and tribological characteristics of Inconel 718. Tribol Int. 2021;163:107178.
[10] De Bartolomeis A, Newman ST, Jawahir IS, Biermann D, Shokrani A. Future research directions in the machining of Inconel 718. J Mater Process Technol. 2021;297:117260.
[11] Sivaiah P, Ajay Kumar GV, Singh MM, Kumar HV, Ajay Kumar G, Singh M, et al. Effect of novel hybrid texture tool on turning process performance in MQL machining of Inconel 718 superalloy. Mater Manuf Process. 2019;35(1):61–71.
[12] Paswan K, Pramanik A, Chattopadhyaya S. Machining performance of Inconel 718 using graphene nanofluid in EDM. Mater Manuf Process. 2020;35(1):33–42.
[13] Sivalingam V, Zhao Y, Thulasiram R, Sun J, kai G, Nagamalai T. Machining behaviour, surface integrity and tool wear analysis in environment friendly turning of Inconel 718 alloy. Measurement. 2021;174:109028.
[14] Swamy N, Nanjundeswaraswamy TS, Nyamannavar S. Using Taguchi approach optimization of surface roughness and cutting tool flank wear in turning and drilling operations. GIS Sci J. 2020;7:1197–208.
[15] Pandian PP, Rout IS. Parametric investigation of machining parameters in determining the machinability of Inconel 718 using taguchi technique and grey relational analysis. Procedia Comput Sci. 2018;133:786–92.
[16] Kitagawa T, Kubo A, Maekawa K. Temperature and wear of cutting tools in high-speed machining of Inconel 718 and Ti6Al6V2Sn. Wear. 1997;202(2):142–8.
[17] Mahesh K, Philip JT, Joshi SN, Kuriachen B. Machinability of Inconel 718: a critical review on the impact of cutting temperatures. Mater Manuf Process. 2021;36(7):753–91.
[18] Kartheek G, Srinivas K, Devaraj C. Optimization of residual stresses in hard turning of super alloy Inconel 718. Mater Today Proc. 2018;5(2):4592–600.
[19] Tebassi H, Yallese MA, Khettabi R, Belhadi S, Meddour I, Girardin F. Multi-objective optimization of surface roughness, cutting forces, productivity and power consumption when turning of Inconel 718. Int J Ind Eng Comput. 2016;7:111–34.
[20] Ramesh S, Viswanathan R, Ambika S. Measurement and optimization of surface roughness and tool wear via grey relational analysis. TOPSIS RSA Tech Meas. 2016;78:63–72.
[21] Ma W, Wang FJ, Jia ZY, Gao YY. Machining parameter optimization in high-speed milling for Inconel 718 curved surface. Mater Manuf Process. 2015;31(13):1692–9.
[22] Pekşen H, Kalyon A. Optimization and measurement of flank wear and surface roughness via Taguchi based grey relational analysis. Mater Manuf Process. 2021;36(16):1865–74.
[23] Schirra JJ. Effect of heat treatment variations on the hardness and mechanical properties of wrought Inconel. TMS. 1997;718:625–706.
[24] Skerlos SJ, Hayes KF, Clarens AF, Zhao F. Current advances in sustainable metalworking fluids research. Int J Sustain Manuf. 2008;1(1/2):180.
[25] Sarıkaya M, Güllü A. Multi-response optimization of minimum quantity lubrication parameters using Taguchi-based grey relational analysis in turning of difficult-to-cut alloy Haynes 25. J Clean Prod. 2015;91:347–57.
[26] Benardos PG, Vosniakos GC. Predicting surface roughness in machining: a review. Int J Mach Tools Manuf. 2003;43(8):833–44.
[27] Qehaja N, Jakupi K, Bunjaku A, Bruçi M, Osmani H. Effect of machining parameters and machining time on surface roughness in dry turning process. Procedia Eng. 2015;100:135–40.
[28] Pawade RS, Joshi SS. Multi-objective optimization of surface roughness and cutting forces in high-speed turning of Inconel 718 using Taguchi grey relational analysis (TGRA). Int J Adv Manuf Technol. 2011;56(1–4):47–62.

[29] Khanna N, Agrawal C, Dogra M, Pruncu CI. Evaluation of tool wear, energy consumption, and surface roughness during turning of inconel 718 using sustainable machining technique. J Mater Res Technol. 2020;9(3):5794–804.
[30] Xavior MA, Manohar M, Jeyapandiarajan P, Madhukar PM. Tool wear assessment during machining of Inconel 718. Procedia Eng. 2017;174:1000–8.
[31] Pinheiro C, Kondo MY, Amaral SS, Callisaya ES, De Souza JV, De Sampaio Alves MC, et al. Effect of machining parameters on turning process of Inconel 718. Mater Manuf Process. 2021;36(12):1421–37.
[32] Akkurt I. Effective atomic numbers for Fe–Mn alloy using transmission experiment. Chin Phys Lett. 2007;24(10):2812–4.
[33] Ural A, Kilimci ZH. The prediction of chiral metamaterial resonance using convolutional neural networks and conventional machine learning algorithms. Int J Comput Exp Sci Eng. 2021;7(3):156–63.
[34] Akkurt I. Effective atomic and electron numbers of some steels at different energies. Ann Nucl Energy. 2009;36(11–12):1702–5. doi: 10.1016/j.anucene.2009.09.005.
[35] Caymaz T, Çalışkan S, Botsalı AR. Evaluation of ergonomic conditions using fuzzy logic in a metal processing plant. Int J Comput Exp Sci Eng. 2022;8(1):19–24.
[36] ALMisned G, Sen Baykal D, Kilic G, Susoy G, Zakaly HM, Ene A, et al. Assessment of the usability conditions of Sb_2O_3–PbO–B_2O_3 glasses for shielding purposes in some medical radioisotope and a wide gamma-ray energy spectrum. Appl Rheol. 2022;32(1):178–89.
[37] Arbouz H. Modeling of a tandem solar cell structure based on CZTS and CZTSe absorber materials. Int J Comput Exp Sci Eng. 2022;8(1):14–8.
[38] Çilli A, Beken M, Kurt N. Determination of theoretical fracture criteria of layered elastic composite material by ANFIS method from artificial intelligence. Int J Comput Exp Sci Eng. 2022;8(2):32–9.
[39] ALMisned G, Sen Baykal D, Susoy G, Kilic G, Zakaly HM, Ene A, et al. Determination of gamma-ray transmission factors of WO_3–TeO_2–B_2O_3 glasses using MCPX Monte Carlo code for shielding and protection purposes. Appl Rheol. 2022;32(1):166–77. doi: 10.1515/arh-2022-0132.
[40] Waheed F, İmamoğlu M, Karpuz N, Ovalıoğlu H. Simulation of neutrons shielding properties for some medical materials. Int J Comput Exp Sci Eng. 2022;8(1):5–8.
[41] Safiddine S, Amokrane K, Debieb F, Soualhi H, Benabed B, Kadri E. How quarry waste limestone filler affects the rheological behavior of cement-based materials. Appl Rheol. 2021;31(1):63–75.
[42] Şen Baykal D, Tekin H, Çakırlı Mutlu R. An investigation on radiation shielding properties of borosilicate glass systems. Int J Comput Exp Sci Eng. 2021;7(2):99–108.
[43] Tan T, Zhao Y, Zhao X, Chang L, Ren S. Mechanical properties of sandstone under hydro-mechanical coupling. Appl Rheol. 2022;32(1):8–21.
[44] Tekin HO, Cavli B, Altunsoy EE, Manici T, Ozturk C, Karakas HM. An investigation on radiation protection and shielding properties of 16 slice computed tomography (CT) facilities. Int J Comput Exp Sci Eng. 2018;4(2):37–40. doi: 10.22399/ijcesen.408231
[45] Sarihan M. Simulation of gamma-ray shielding properties for materials of medical interest. Open Chem. 2022;20(1):81–7.
[46] Demir N, Kıvrak A, Üstün M, Cesur A, Boztosun I. Experimental study for the energy levels of europium by the clinic LINAC. Int J Comput Exp Sci Eng. 2017;3(1):47–9.
[47] Karaali R, Keven A. Evaluation of four different cogeneration cycles by using some criteria. Appl Rheol. 2022;32(1):122–37.
[48] Arslankaya S, Çelik MT. Prediction of heart attack using fuzzy logic method and determination of factors affecting heart attacks. Int J Comput Exp Sci Eng. 2021;7(1):1–8.
[49] Ayhan E. Structural, physical, and mechanical properties of the TiO_2 added hydroxyapatite composites. Open Chem. 2022;20(1):272–6.
[50] Bekir O. Gamma-ray shielding properties of Nd_2O_3 added iron–boron–phosphate based composites. Open Chem. 2022;20(1):237–43.
[51] Salima B, Seloua D, Djamel F, Samir M. Structure of pumpkin pectin and its effect on its technological properties. Appl Rheol. 2022;32(1):34–55.
[52] Özseven A. Assessment of using electronic portal imaging device for analysing bolus material utilised in radiation therapy. Open Chem. 2022;20(1):61–8.